Offset Bin Classification Network for Accurate Object Detection

Heqian Qiu, Hongliang Li[*], Qingbo Wu, Hengcan Shi
University of Electronic Science and Technology of China
Chengdu, China
hqqiu@std.uestc.edu.cn, hlli@uestc.edu.cn, qbwu@uestc.edu.cn, shihc@std.uestc.edu.cn

Abstract

Object detection combines object classification and object localization problems. Most existing object detection methods usually locate objects by leveraging regression networks trained with $Smooth\ L_1$ loss function to predict offsets between candidate boxes and objects. However, this loss function applies the same penalties on different samples with large errors, which results in suboptimal regression networks and inaccurate offsets. In this paper, we propose an offset bin classification network optimized with cross entropy loss to predict more accurate offsets. It not only provides different penalties for different samples but also avoids the gradient explosion problem caused by the samples with large errors. Specifically, we discretize the continuous offset into a number of bins, and predict the probability of each offset bin. Furthermore, we propose an expectation-based offset prediction and a hierarchical focusing method to improve the prediction precision. Extensive experiments on the PASCAL VOC and MS-COCO datasets demonstrate the effectiveness of our proposed method. Our method outperforms the baseline methods by a large margin.

1. Introduction

Object detection is a fundamental yet challenging computer vision task, which includes object classification and object localization problems. A broad set of computer vision applications, such as autonomous driving [7, 17, 39–41], video surveillance [6, 24] and robotics [38, 42, 45] will benefit from accurate object localization.

Most of state-of-the-art object detection methods [1, 8, 11, 12, 20, 21, 26, 30, 31, 35, 44] firstly generate a series of candidate boxes and then predict offsets for these boxes to locate objects, as shown in Figure 1 (a). Since offsets are continuous values, these methods predict them by leveraging regression networks that are optimized using the L_2 or $Smooth\ L_1$ losses. However, as investigated by [9], the L_2 loss [10] may cause gradient explosions when there are large offset errors. To avoid this problem, the $Smooth\ L_1$ loss [9] weakens the effects of the samples with large errors by clipping their gradients. Although the $Smooth\ L_1$ loss solves the gradient explosion problem, it cannot penalize enough the samples with large errors, which results in suboptimal regression networks and inaccurate offsets between candidate boxes and objects. For example, in Figure 1 (a), the train object can not be tightly surrounded by a bounding box.

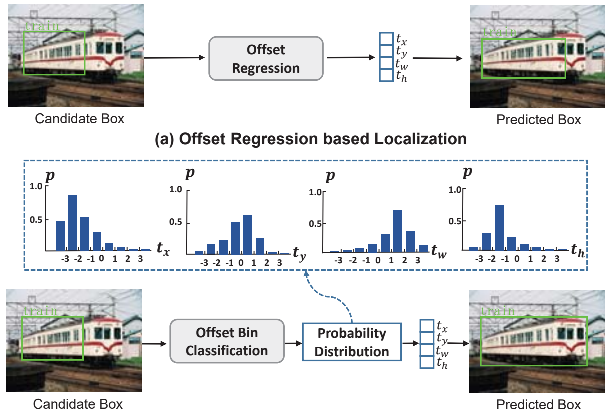

(a) Offset Regression based Localization

(b) Offset Bin Classification based Localization

Figure 1. A comparison of typical offset regression based object detection method and our proposed offset bin classification method. (a) The typical object detection method locates objects based on offset regression. (b) The proposed method locates objects based on the output probability distribution over different offset bins. The typical offset regression method make limited offsets from the candidate box towards the object, whereas this problem is avoided by the offset bin classification method.

To address this problem, we propose an offset bin classification network to predict more accurate offsets, as shown in Figure 1 (b). The proposed method adopts a classification network trained with a cross entropy loss rather than a $Smooth\ L_1$ or L_2 loss. On the one hand, it gives samples with different offset errors adequate penalties. On the

[*]Corresponding author.

偏移垃圾箱分类网络，用于精确对象检测

Heqian Qiu, Hongliang Li , Qingbo Wu, Hengcan Shi University
of Electronic Science and Technology of China Chengdu, China
hqqiu@std.uestc.edu.cn, hlli@uestc.edu.cn, qbwu@uestc.edu.cn, shihc@std.uestc.edu.cn

Abstract

对象检测结合了对象分类和OB−JECT本地化问题。大多数现有物体检测方法通常通过利用具有平滑L1损耗函数的回归网络训练来定位对象，以预测候选框和对象之间的开关。但是，此损失函数在具有大错误的不同样本上应用相同的惩罚，从而导致次优回归网络和不准确的偏移。在本文中，我们提出了一种偏移箱分类网络，其优化了跨熵损耗来预测更准确的偏移。它不仅为不同的样本提供了不同的惩罚，还避免了由大错误引起的渐变爆炸问题。具体地，我们将持续的偏移离散到多个箱中，并预测每个偏移箱的概率。此外，我们提出了基于期望的偏移预测和分层聚焦方法来提高预测精度。在Pascal VOC和MS−Coco数据集上的广泛实验证明了我们所提出的方法的有效性。我们的方法通过大的边距来实现基线方法。

1. Introduction

对象检测是一个基本且挑战的愿景任务，包括对象分类和对象本地化问题。一组广泛的计算机振动应用，如自主驾驶[7,17,39−41]，视频监控[6,24]和机器人[38,42,45]将受益于准确的对象本地化。大多数最先进的对象检测方法[1,8,11,12,20,21,26,30,31,35,44]首先生成一系列候选盒，然后预测这些盒子的偏移找到对象，如图1（a）所示。由于偏移是连续值，因此这些方法通过使用L2或平滑的L1损耗优化的杠杆作用回归网络来预测它们。但是，如[9]所研究，

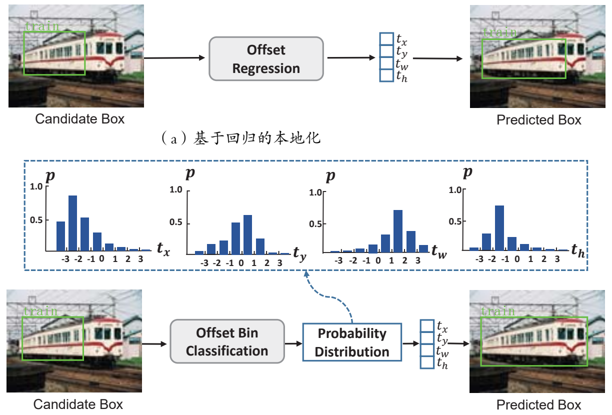

（a）基于回归的本地化

（b）基于offset bin分类的本地化

图1.基于典型的偏移回归的ob−ject检测方法和我们提出的偏移箱分类方法的比较。（a）典型的对象检测方法基于偏移回归定位对象。（b）所提出的方法根据不同的偏移箱上的输出概率分布定位ob−jects。典型的偏移回归方法从候选盒朝向物体中的有限偏移，而偏移箱分类方法避免了该问题。L.

2丢失[10]可能导致偏移误差时造成梯度爆炸。为了避免这个问题，平滑的L1损失[9]通过剪切它们的梯度，削弱了样本与大误差的影响。虽然光滑的L1损失解决了梯度爆炸问题，但它不能惩罚具有大错误的样本，这导致候选盒和对象之间的次优回归网络和不准确的偏移。例如，在图1（a）中，列车物体不能被边界框紧密包围。为了解决这个问题，我们提出了一个偏移的垃圾箱分类网络来预测更准确的偏移，如图1（b）所示。所提出的方法采用具有跨熵损耗的分类网络，而不是平滑的L1或L2损耗。一方面，它给出了不同的偏移错误足够的惩罚。在这一点

[*]Corresponding author.

other hand, it avoids the gradient explosion problem. Nevertheless, the classification network can only predict discrete offset values. Therefore, we propose an expectation-based offset prediction and a hierarchical focusing offset prediction to further improve the prediction precision.

Specifically, we quantize the continuous offset into a number of bins using the uniform discretization and then train an offset bin classification network with a cross entropy loss to predict the probability distribution of offset bins. Inspired by [37], we turn the classification results into the object location by calculating the softmax expected value of discretized offset bins. Meanwhile, we propose a hierarchical focusing offset prediction network to gradually refine offset bins for more precise object localization. We validate the effectiveness of our method on two common object detection datasets, including the PASCAL VOC and MS-COCO datasets. The results show that our proposed method is beneficial to accurate object detection.

Our contributions can be summarized as follows:

• We propose an offset bin classification network to predict more accurate offsets instead of regression networks optimized by $Smooth\ L_1$ or L_2 loss.

• To further produce more precise object localization, we propose an expectation-based offset prediction and a hierarchical focusing offset prediction.

• Extensive experiments on two common datasets demonstrate the effectiveness of the proposed methods.

2. Related Work

Object Detectors: Modern object detection frameworks usually can be classified as two-stage and single-stage detectors. In two-stage detectors [1, 8, 11, 12, 20, 21, 26, 30, 31, 35, 44], a sparse set of region proposals that may contain objects are first generated, and then their features are extracted for the following classification and localization. The representative methods, including Faster R-CNN [35], FPN [20] and Mask R-CNN [12], have achieved dominated performance on various benchmarks. Compared with two-stage detectors, single-stage detectors [18, 19, 21, 23, 32–34] reach high inference speed, such as YOLO [32–34], SSD [23], RetinaNet [21]. They usually skip the region proposal generation step and directly predict bounding boxes following the anchor box scheme. Although these methods have detected objects successfully, it is still a challenging problem to achieve accurate object localization.

Bounding Box Regression: In order to solve the problem of object localization, most of object detection methods [1, 8–11, 15, 26, 28, 44] leverage bounding box regression networks to predict offsets of four coordinates that transform candidate boxes to objects. R-CNN [10] predicted these offsets by training a linear regression model with L_2 loss. However, it is easy to cause gradient explosion when there are some samples with large errors. Replacing L_2 loss, Fast R-CNN [9] proposed $Smooth\ L_1$ loss to reduce the effects of the samples with large errors, which has been widely accepted for regression in object detection. Balanced L1 loss [28] further increased the gradient contribution of the samples with small errors to rebalance the the involved classification and localization tasks as well as samples with different attributes. A different approach KL loss [14] took the ambiguities of ground truth bounding boxes into account and learned bounding box regression and localization variance for more accurate object localization. In addition, UnitBox [46] and GIoU [36] directly used the evaluation metric as object functions to address the gap between optimizing the commonly used distance loss and maximizing metric values. However, it is hard to optimize different bounding boxes with the same IoU.

In addition, a series of object detectors [1, 8, 11, 26, 44] attempt to improve the object localization by iteratively regressing bounding boxes. They both cascaded multiple regressors and fed the detection results after each iteration into the next bounding box regressor. Cascade R-CNN [1] considered the distribution of detection outputs and resampled bounding boxes at each iteration to guarantee the matching between the quality of detector and that of testing. However, it is non-monotonic to improve the location accuracy as the number of iterations increases. IoU-Net [15] proposed to predict the IoU with matched groundtruth as the localization confidence to guide the regression of bounding box. Instead of regression network, we propose an offset bin classification network with a cross entropy loss to achieve more accurate object localization, which is also effectively turned in other computer vision areas. For example, [27] predicted the detection heatmaps and the associative embedding tags for human pose estimation. [5] trained a depth estimation network by using an ordinal regression loss instead of a L_2 loss.

Recently, some anchor-free methods [16, 43, 47] directly predict the heatmaps of keypoints of bounding boxes, and introduce different kinds of loss functions to refine and group these keypoints for the final detected bounding boxes. CornerNet [16] used a SmoothL1 loss to regress the local offsets, and pull loss and push loss to constrain the distances between keypoints. CenterNet [47] regressed localization offset and object size using two L1 loss functions. FCOS [43] employed an IoU loss to regress the area of bounding box. Unlike the proposed method, they usually require carefully group keypoints for final objects.

3. Approach

In this section, we first review and analyze the problem of the conventional bounding box regressors. Then, we introduce our proposed offset bin classification network to address this problem, which is implemented based on popular FPN [20].

另一方面，它避免了梯度爆炸问题。从来没有 -分类网络只能预测离散的偏移值。因此，我们提出了基于期望的偏移预测和分层聚焦偏移偏移，以进一步提高预测精度。具体地，我们使用均匀的离散化量化连续偏移到多个箱中，然后用交叉电阻丢失训练偏移箱分类网络以预测偏移箱的概率分布。灵感来自[37]，通过计算离散化偏移箱的Softmax预期值，将分类结果转换为对象位置。同时，我们提出了一个分层聚焦偏移预测网络，以逐渐改进偏移箱，以获得更精确的对象本地化。我们验证了我们对两个公共对象检测数据集的方法的有效性，包括Pascal VOC和MS−Coco数据集。结果表明，我们提出的方法有利于准确的对象检测。我们的贡献可以归纳如下：　我们提出了一个偏移垃圾箱分类网络，以预先描述更准确的偏移而不是通过平滑L1或L2损耗优化的回归网络。

为了进一步产生更精确的对象本地化，我们提出了基于期望的偏移预测和Hierar− Chical聚焦偏移预测。

两个常见数据集上的广泛实验证明了所提出的方法的有效性。

2. Related Work

对象探测器：现代物体检测框架通常可以被归类为两级和单级的解决方案。在两阶段检测器中[1,8,11,12,20,21,26,30,31,35,44]，首先产生可能包含Ob−Jepts的稀疏区域提案集，然后它们的特征是提取以下分类和本地化。代表性方法，包括更快的R−CNN [35]，FPN [20]和掩模R−CNN [12]，已经在各种基准上实现了主导的性能。与两级探测器相比，单级探测器[18,19,21,23,32−34]达到高推理速度，例如yolo [32−34]，SSD [23]，视网膜[21]。它们通常跳过区域提案基因，并直接在锚箱方案之后预测边界框。虽然这些方法已成功进行了对象，但实现了准确对象本地化仍然是一个具有挑战性的问题。绑定框回归：为了解决对象本地化的问题，大多数物体检测方法[1,8−11,15,26,28,44]利用边界框重新定位网络预测四个将候选框转换为对象的坐标。 R−CNN [10]通过培训具有L2损耗的线性回归模型来预测这些偏移。但是，当有一些具有大错误的样本时，很容易引起梯度利用。换 -

L2损失，FAST R−CNN [9]提出平滑L1损失，以减少样品的效果大的误差，这已被广泛接受对象检测中的回归。平衡L1丢失[28]进一步提高了样本的渐变贡献，以小错误来重新平衡所涉及的分类和本地化任务以及具有不同属性的样本。不同的方法KL丢失[14]将地面真理界限框架的含糊存在，并学习了更多准确对象本地化的界限框回归和本地化方差。此外，Unitbox [46]和Giou [36]直接使用评估度量作为对象函数来解决优化常用距离损耗和最大化度量值之间的间隙。但是，很难用同样的IOU优化不同的边界框。此外，一系列对象检测器[1,8,11,26,44]试图通过迭代地重复束缚绑定框来改善对象定位。它们都级联多个重新格雷斯，并在每次迭代到下一个边界框回归线后喂养检测结果。 Cascade R−CNN [1]考虑了在每次迭代时检测输出的分布和再采样的边界框，以保证检测器质量与测试之间的匹配。然而，随着迭代的数量增加，它是非单调的，以提高基因准确性。 iou−net [15]建议预测IOU与匹配的基础是指导边界框的回归的本地化信心。我们提出了一个偏移垃圾箱分类网络，跨熵丢失来实现更准确的对象本地化，这也是有效地转动其他计算机视觉区域。对于考试，[27]预测检测热量和用于人类姿势估计的关联嵌入标签。 [5]通过使用序数回归损耗而不是L2损耗训练深度估计网络。最近，一些无锚方法[16,43,47]直接预测边界框的关键点的热量，并引入不同种类的损耗函数来细化和组用于最终检测到的边界框的这些关键点。 Cornernet [16]使用ShimpleL1丢失来分配本地偏移，并拉出损耗并推动丢失，以限制关键点之间的差异。 CenterNet [47]使用两个L1损耗功能回归局部偏移和对象大小。 FCOS [43]使用IOU丢失来分配边界框的区域。与所提出的方法不同，它们通常需要仔细组用于最终对象的关键点。

3. Approach

在本节中，我们首先审查和分析传统边界框回归的问题。然后，我们引发了我们建议的偏移垃圾箱分类网络以遵守这个问题，这是基于流行的FPN [20]实现的。

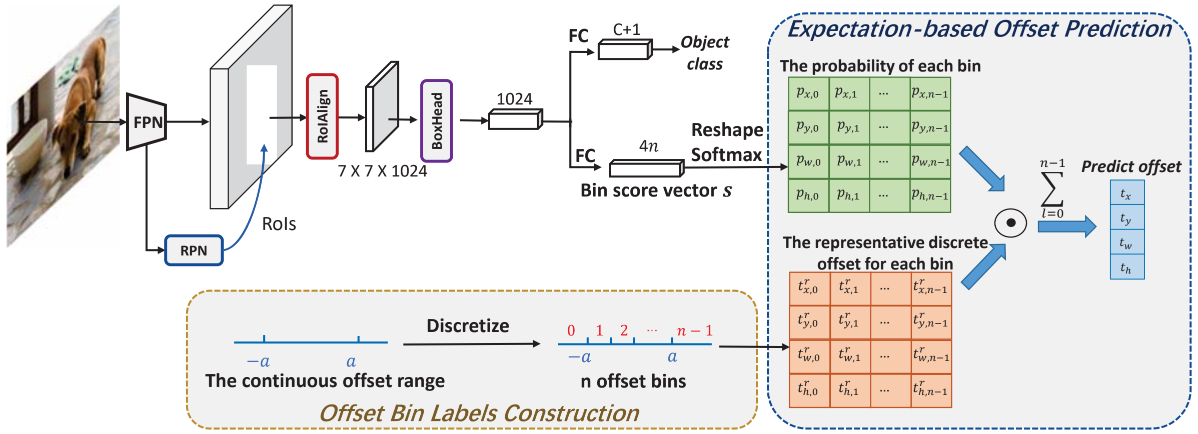
FPN
RPN
RoIs
RoIAlign
7 X 7 X 1024
BoxHead
1024
FC
C+1
Object class
FC
4n
Bin score vector s
Reshape
Softmax
Expectation-based Offset Prediction
The probability of each bin
$p_{x,0}$ $p_{x,1}$ ··· $p_{x,n-1}$
$p_{y,0}$ $p_{y,1}$ ··· $p_{y,n-1}$
$p_{w,0}$ $p_{w,1}$ ··· $p_{w,n-1}$
$p_{h,0}$ $p_{h,1}$ ··· $p_{h,n-1}$
The representative discrete offset for each bin
$t^r_{x,0}$ $t^r_{x,1}$ ··· $t^r_{x,n-1}$
$t^r_{y,0}$ $t^r_{y,1}$ ··· $t^r_{y,n-1}$
$t^r_{w,0}$ $t^r_{w,1}$ ··· $t^r_{w,n-1}$
$t^r_{h,0}$ $t^r_{h,1}$ ··· $t^r_{h,n-1}$
$\odot$
$\sum_{l=0}^{n-1}$
Predict offset
t_x t_y t_w t_h
Discretize
$-a$ a
The continuous offset range
0 1 2 ··· $n-1$
$-a$ a
n offset bins
Offset Bin Labels Construction

Figure 2. The overall architecture of our proposed offset bin classification method for object detection. It consists of three main parts: RoI features extraction, offset bin labels construction and expectation-based offset prediction. The RoI features are extracted by the backbone network FPN [20]. The offset bin labels construction is to discretize the continuous offset range to several offset bins. The expectation-based offset predict is used to turn the classification results to offset estimation by calculating a expected value.

3.1. Revisiting Bounding Box Regression

Let (x, y, w, h) be the center coordinates of bounding box and its width and height. Following R-CNN [10], the common methods leverage regression networks to learn offsets that transform candidate boxes to ground-truth boxes. They parameterize the offsets of four coordinates as follows:

$$\begin{aligned} t_x &= (x - x_a)/w_a, t_y = (y - y_a)/h_a \\ t_w &= log(w/w_a), t_h = log(h/h_a) \\ t_x^* &= (x^* - x_a)/w_a, t_y^* = (y^* - y_a)/h_a \\ t_w^* &= log(w^*/w_a), t_h^* = log(h^*/h_a) \end{aligned} \tag{1}$$

where t_x, t_y, t_w, t_h are the predicted offsets, $t_x^*, t_y^*, t_w^*, t_h^*$ are the target offsets. x, x^* and x_a (likewise for y, w and h) are from the predicted box, ground-truth box and the candidate box (anchor or proposal box) respectively. The goal is to minimize the errors between the predicted and target offsets:

$$L_{loc} = \sum_{i \in \{x,y,w,h\}} L_{reg}(t_i - t_i^*) \tag{2}$$

where L_{reg} is squared-error L_2 loss function in R-CNN [10]. However, it is sensitive to some samples when there is a large offset errors.

Replacing L_2 loss, Fast R-CNN [9] adopts $Smooth\ L_1$ loss function to evade the above problem:

$$Smooth\ L_1(x) = \begin{cases} \frac{x^2}{2\beta}, & |x| \leq \beta \\ |x| - \frac{\beta}{2}, & otherwise \end{cases} \tag{3}$$

$$\frac{\partial Smooth\ L_1}{\partial t_i} = \frac{\partial Smooth\ L_1}{\partial x} \begin{cases} \frac{x}{\beta}, & |x| \leq \beta \\ sgn(x), & otherwise \end{cases} \tag{4}$$

where the deviation $x = t_i - t^*$, β is usually set to 1 in two-stage detectors. sgn represents symbolic function. Note that the samples with the offset error larger than β are forced to clip the gradients to 1 or -1 for reducing their effects, causing insufficient penalty for these samples. So, the regression networks optimized by the $Smooth\ L_1$ loss function predict inaccurate offsets between candidate boxes and objects.

3.2. Offset Bin Classification Network

To address this problem, we propose an offset bin classification network to achieve more accurate object localization. The overall architecture of the proposed method is illustrated in Figure 2. Given an image, we first generate a sparse set of candidate boxes using Region Proposal Network (RPN) [20] and then extract these RoIs features from the image feature maps obtained by feature pyramid networks (FPN) [20]. Based on the extracted RoI features, we predict their corresponding object categories and offset bin confidence scores instead of concrete offset values. Moreover, we use the expectation-based offset prediction and the hierarchical focusing offset prediction in Figure 3 to further improve the precision of predicted offsets.

3.2.1 Offset Bin Labels Construction

As shown in Figure 4, we quantize the continuous offset in Section 3.1 into a set of representative discrete offsets. Divide the offset range $(-a, a)$ uniformly into m non-overlapping bins. The width w of each bin in the range $(-a, a)$ is $\frac{2a}{m}$. In addition, we also separately divide the range $(-\infty, -a]$ and $[a, +\infty)$ into two bins. Thus, the total number of bins is denoted as $n = m + 2$. The discrete bin labels are denoted as $L \in \{0, 1, ..., n-1\}$. The representa-

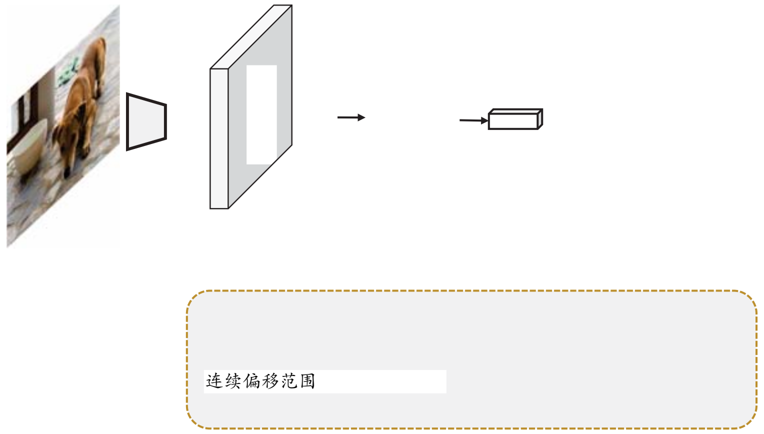

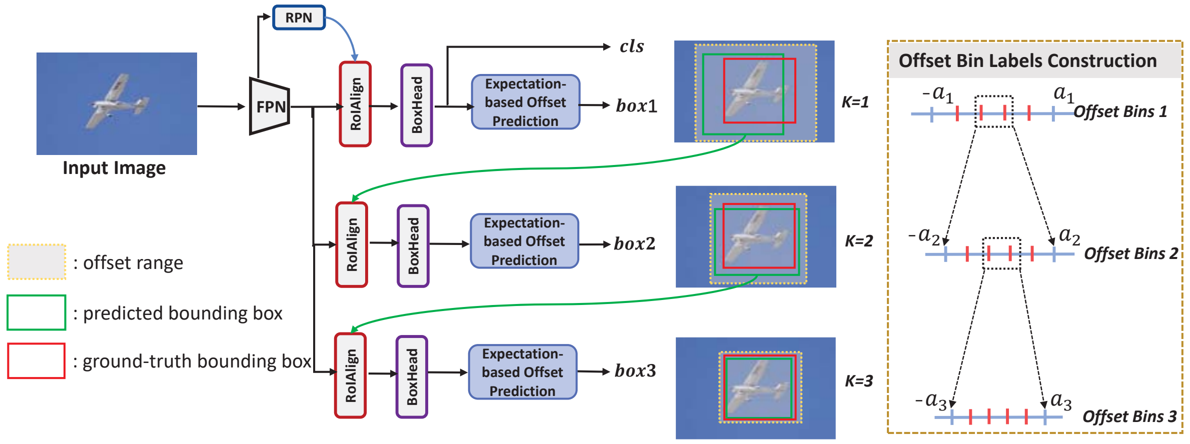

Figure 3. The architecture of the proposed hierarchical focusing offset prediction. Here, we show three stages in the hierarchical focusing offset prediction. Yellow dashed boxes filled with gray denote the offset range in each stage. Green boxes and red boxes represent predicted boxes and ground-truth boxes in each stage. The offset range in each stage is defined within the offset bins of previous stage.

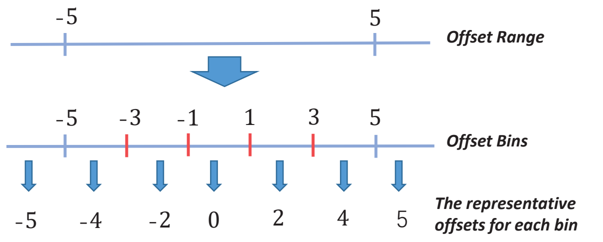

Figure 4. Illustration of offset bin construction. The offset range $-5, 5)$ is uniformly discretized into five bins, and the median values of each bin stand for their representative offsets. In addition, the range $(-\infty, -5]$ and $[5, +\infty)$ uses the endpoint -5 and 5 as their representative offset, respectively.

tive offset for each bin can be indicated as follows:

$$t^r_{i,l} = \begin{cases} -a + (l + \frac{1}{2}) * w & l \in [0, m] \\ -a & l = m + 1 \\ a & l = m + 2 \end{cases} \quad (5)$$

where $t^{r,l}$ is the representative offset corresponding to the bin label l for the coordinate i of the bounding box. The representative offsets for the labels from 0 to m are expressed as the median value of each bin, and the other labels are expressed as the offset of the endpoint.

3.2.2 Network Learning

Based on the discretized offset bin labels, it is straightforward to cast the object localization as the multi-class classification problem instead of directly regression. As shown in Figure 2, the candidate box is fed into the BoxHead of backbone network FPN [20] to generate its offset bin score vector $s \in R^{4n}$, where 4 is the four coordinates of the bounding box, n is the number of offset bins. Then we reshape the score vector to $R^{4\times n}$ and normalize respectively the score vector of each coordinate into the form of probability by a softmax function as follows:

$$p_{i,l} = \frac{exp(s_{i,l})}{\sum_{l=0}^{n-1} exp(s_{i,l})} \quad (6)$$

where $p_{i,l}$ indicates the probability of the i-th coordinate offset belongs to the l-th bin.

The loss function L_{bin} for the offset bin classifier is formulated as a cross entropy loss:

$$L_{bin}(p_{i,l}, l) = -\sum_{i\in\{x,y,w,h\}} \sum_{l=0}^{n-1} y_l * logp_{i,l} \quad (7)$$

in which the loss is calculated when the ground-truth class is labeled l, where $y_l \in \{0, 1\}$. The gradient with regard to the output score s^b_{il} of the classifier layer can be derived as follows:

$$\frac{\partial L_{bin}}{\partial s_i} = \begin{cases} -\sum_{i\in\{x,y,w,h\}}(p_{i,l} - 1), & y_l = 1 \\ -\sum_{i\in\{x,y,w,h\}}(p_{i,l}), & y_l = 0 \end{cases} \quad (8)$$

Based on the above formula, the gradient is bounded and its norm is limited to $[0, 1]$, which is more stable for all samples compared with L_2 loss function. Meanwhile, it effectively takes into account the samples using different gradient contributions based on the predicted probabilities $p_{i,l}$ compared to $Smooth\ L1$ loss.

To end up, we use the loss function L to end-to-end train our network for accurate object detection:

$$L = L_{cls} + \lambda_{bin} L_{bin} \quad (9)$$

where L_{cls} denotes the loss for classification of objects, The offset bin classification loss L_{bin} is used for localization of objects. λ_{bin} is the weight that control the balance among these losses. In this paper, we set λ_{bin} to 1.

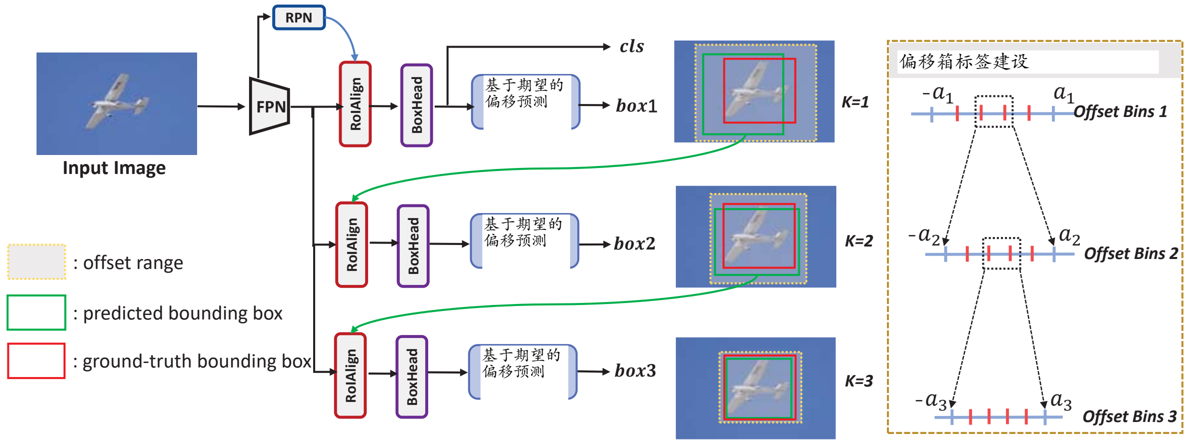

图3.所提出的分层聚焦偏移预测的架构。在这里，我们在分层聚焦偏移预测中显示三个阶段。填充有灰色的黄色虚线盒子表示每个阶段的偏移量程。绿色盒子和红色框代表每个阶段的预测盒子和地面真相盒。每个阶段的偏移量级在前一级的偏移区内定义。

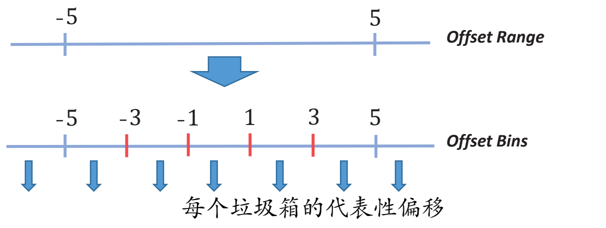

图4.偏移箱施工的插图。偏移范围（−5,5）被均匀地离散化为五个垃圾箱，每个箱子的中位数为他们的代表性偏移。另外，范围（−∞，−5]和[5，+∞）分别使用端点−5和5分别作为其代表性偏移。

每个垃圾箱的Cive偏移可以表示如下：

$$t^r_{i,l} = \begin{cases} -a + (l + \frac{1}{2}) * w & l \in [0, m] \\ -a & l = m + 1 \\ a & l = m + 2 \end{cases} \quad (5)$$

如果TRI，L是对应于绑定框的坐标I的BIN标签L对应的代表性偏移。从0到m的标签的重复偏移被表示为每个箱的中值，另一个标签表示为端点的偏移量。

3.2.2 Network Learning

基于离散化偏移箱标签，将对象本地化作为多级分类问题而不是直接回归是直接的。如图2所示，候选盒被馈送到后骨网络FPN [20]的盒头中，以产生其偏移栅格评分Vec−tor S∈R4n，其中4是界定框的四个坐标，n是偏移垃圾箱的数量。然后我们重塑分数矢量到R4×n并分别通过SoftMax函数分别对每个坐标的分数矢量分别为概率的形式，如下所示：

$$p_{i,l} = \frac{exp(s_{i,l})}{{}_{l=0}^{n-1} exp(s_{i,l})} \quad (6)$$

其中pi，l表示第i个坐标偏移的概率属于l−th bin。偏移箱分类器的损耗功能LBIN作为交叉熵丢失，使：

$$L_{bin}(p_{i,l}, l) = -\sum_{i\in\{x,y,w,h\}} \sum_{l=0}^{n-1} y_l * logp_{i,l} \quad (7)$$

其中计算丢失时，当地面真理类被标记为l，其中yl∈{0,1}。关于输出得分SB的梯度

可以导出分类器层的IL，如下所示：

$$\frac{\partial L_{bin}}{\partial s_i} = \begin{cases} -\sum_{i\in\{x,y,w,h\}}(p_{i,l} - 1), & y_l = 1 \\ -\quad {}_{i\in\{x,y,w,h\}}(p_{i,l}), & y_l = 0 \end{cases} \quad (8)$$

基于上述公式，偏移是有界的，其规范限制为[0,1]，与L2损耗功能相比，所有样品更稳定。同时，它有效考虑了使用基于预测概率Pi，L的不同梯度概要的样本与平滑L1损耗相比。最后，我们使用损失函数l到端到端的列车我们的网络准确对象检测：

$$L = L_{cls} + \lambda_{bin} L_{bin} \quad (9)$$

其中LCL表示对象分类的损失，偏移箱分类丢失Lbin用于对象的本地化。λ Bin是控制这些损失之间平衡的重量。在本文中，我们将λ bin设置为1。

Method	Expectation	Hierarchical	AP	AP_{50}	AP_{60}	AP_{70}	AP_{80}	AP_{90}
Bounding Box Regression [20]			45.0	**74.5**	**69.5**	57.6	36.0	6.6
Bin Classification			45.8	73.3	67.9	57.2	39.6	9.8
Bin Classification	✓		47.5	74.0	69.0	58.8	41.5	13.6
Bin Classification		✓	47.5	72.8	67.9	58.1	42.0	16.0
Bin Classification	✓	✓	**49.0**	73.2	68.4	**59.0**	**44.3**	**19.6**

Table 1. The effects of each component in the proposed method. Results are reported on the VOC2007 *test* set [4]. The baseline method with ResNet-50-FPN [20] locates object by bounding box regression method. Expectation and Hierarchical represent the expectation-based offset prediction and hierarchical focusing offset prediction.

3.2.3 Expectation-based Offset Prediction

Since offsets are continuous values with high precision, the classification network only predicts discrete offset values. Thus, we propose two different methods to improve the precision of detection results: the expectation-based offset prediction and the hierarchical focusing offset prediction.

For the expectation-based offset prediction method in Figure 2, we utilize the probability distribution over different offset bins to estimate the predicted offset t_i, which is calculated by a softmax expected value instead of a max value, as follows:

$$\begin{aligned} t_i &= \mathbb{E}(T_i^r) \\ &= \sum_{l=0}^{n-1}(p_{i,l} * t^r_{i,l}) \end{aligned} \tag{10}$$

where $T_i^r = \{t^r_{i,0}, t^r_{i,1}, ..., t^r_{i,n-1}\}$ denotes the set of representative discrete offsets for n bins. The symbol $\mathbb{E}$ indicates the expectation of discrete offsets.

3.2.4 Hierarchical Focusing Offset Prediction

Furthermore, we propose a hierarchical focusing offset prediction with a coarse-to-fine strategy to gradually refine the bin interval as shown in Figure 3. The discretized value will be closer to the target value when the bin interval is very small. Assume that there are K stages and n_k bins in the k-th stage. In each stage, the offset range $(-a_k, a_k)$ is defined within the offset bins of previous stage. So, the width w_k of bins can be denoted as $\frac{w_{k-1}}{n_k}$. Then, we predict the offset t^k of each stage similar to Section 3.2.3. The final predicted offset can be calculated as:

$$t_i = \sum_{k=1}^{K} t_i^k \tag{11}$$

As shown in Figure 3, in the first stage, we predict offsets between candidate boxes generated by RPN and objects within the offset range $(-a_1, a_1)$. Subsequently, at each stage, we predict finer offsets within the previous offset bin. By progressively classifying offsets, we can obtain more precise bounding boxes.

4. Experiments

To evaluate the effectiveness of the proposed offset bin classification network, we conduct extensive experiments on two standard object detection datasets, including the PASCAL VOC dataset [4] and the MS-COCO dataset [22].

Datasets. The PASCAL VOC dataset [4] contains 20 object categories, which consists of the PASCAL VOC2007 dataset and the PASCAL VOC2012 dataset. Following [35], we train our network on the union of VOC 2007 *trainval* and VOC2012 *trainval* sets, including 5011 and 11540 images, respectively, and evaluate on the VOC2007 *test* set containing 4952 images. The MS-COCO dataset [22] involves 80 object categories, which has larger scale than the PASCAL VOC dataset. Following the common practice [20, 28], we use the *train-2017* set with 115K images for training and report the final results on the *test-dev* set with 20k images.

Evaluation Metrics. We adopt the standard COCO-style Average Precision (AP) to measure the detection performance of various qualities, which averages mAP across different IoU thresholds from 0.5 to 0.95 with an interval of 0.05. It also includes AP across small scale AP_S, medium scale AP_M and large scale AP_L.

Implementation Details. For fair comparison, we implement all experiments based on PyTorch [29] and MMDetection [2]. We employ FPN [20] based on ResNet-50 and ResNet-101 [13] as the baseline networks. Following the typical convention, we adopt the input image scale of 1000 × 600 on the PASCAL VOC dataset [4] and a scale of 1333 × 800 on the MS-COCO dataset [22]. We train detectors end-to-end with 2 GPUs (2 images per GPU) for 12 epoch. The initial learning rate is set to 0.005 and decreased by a factor 0.1 after 8 epochs and 11 epochs. Unless otherwise specified, all other hyper-parameters follow the default settings in MMDetection [2]. The loss weights λ_{bin} are set to 1. The offset range a and the number of bins n are set to 3 and 20, respectively. In the hierarchical focusing offset prediction, the number of stages K is set to 2.

4.1. Ablation Study

In this section, we validate the effectiveness on the baseline ResNet-50-FPN [20]. Without loss generality, we per-

方法期望分层AP50 AP60 AP70 AP80 AP90								
Bounding Box Regression [20]			45.0	**74.5**	**69.5**	57.6	36.0	6.6
Bin Classification			45.8	73.3	67.9	57.2	39.6	9.8
Bin Classification	✓		47.5	74.0	69.0	58.8	41.5	13.6
Bin Classification		✓	47.5	72.8	67.9	58.1	42.0	16.0
Bin Classification	✓	✓	**49.0**	73.2	68.4	**59.0**	**44.3**	**19.6**

表1.每个组分在所提出的方法中的影响。结果是在VOC2007测试集[4]上报告。具有Reset−50−FPN [20]的基线方法通过边界框回归方法定位对象。期望和分层代表基于期望的偏移预测和分层聚焦偏移预测。

3.2.3 Expectation-based Offset Prediction

由于偏移是具有高精度的连续值，因此分类网络仅预测离散偏移值。因此，我们提出了两种不同的方法来提高检测结果的预测：基于期望的偏移预测和分层聚焦偏移预测。对于图2中的基于期望的偏移预测方法，我们利用不同偏移偏移频率的概率分布来估计预测的偏移Ti，其由SoftMax预期值而不是最大值计算，如下所示：

$$\begin{aligned} t_i &= \mathbb{E}(T_i^r) \\ &= \sum_{l=0}^{n-1}(p_{i,l} * t^r_{i,l}) \end{aligned} \tag{10}$$

其中t r i = {tr i，0，tr i，1，...，tr i，n−1}表示n个垃圾箱的一组代理离散偏移。符号E表示离散偏移的期望。

3.2.4分层聚焦偏移预测

此外，我们提出了一种分层聚焦偏移预测，具有粗细的策略，逐渐改进箱间隔，如图3所示。当BIN间隔非常小时，离散值将更接近目标值。假设K−TH阶段有K阶段和NK箱。在每个阶段，偏移范围（−AK，AK）定义在前一级的偏移区内。所以，距离的宽度Wk可以表示为WK−1

NK。然后，我们预测每个阶段的偏移TKI类似于第3.2.3节。最终预测的偏移可以计算为：

$$t_i = \sum_{k=1}^{K} t_i^k \tag{11}$$

如图3所示，在第一阶段，我们预测RPN生成的候选框之间的摘录和偏移范围内的OBECTS（−A1，A1）。随后，在每个阶段，我们预测先前的禁区内的更精细的偏移。通过逐步分类偏移，我们可以获得更精确的边界框。

4. Experiments

为了评估所提出的偏移垃圾箱分类网络的有效性，我们对两个标准对象检测数据集进行了广泛的实验，包括Pascal VOC数据集[4]和MS−Coco DataSet [22]。数据集。 Pascal VOC数据集[4]包含20个OB−JECT类别，其中包括Pascal VOC2007数据集和Pascal VOC2012数据集。以下[35]，我们在VOC 2007 TrainVal和VOC2012 TrainVal集合上培训我们的网络，其中包括5011和11540张图像，并评估包含4952图像的VOC2007测试集。MS−Coco DataSet [22]涉及80个对象类别，其具有比Pascal VOC数据集更大的刻度。在常见的做法之后评估指标。我们采用标准的Coco风格的平均精度（AP）来测量各种质量的检测性能，其平均地图跨越0.5至0.95的阈值，间隔为0.05。它还包括小规模AP，中等尺度APM和大型APL跨的AP。实施细节。为了进行公平比较，我们实现了基于Pytorch [29]和MMDE−TECTION的所有实验[2]。基于Reset−50和Resnet−101 [13]作为基线网络，我们使用FPN [20]。在典型的约定之后，我们在Pascal VOC数据集[4]上采用1000 × 600的输入图像比例，以及MS−Coco DataSet上的1333 × 800的比例[22]。我们培训结束于结束的结果，以2个GPU（每GPU 2张图像）为12时代。初始学习速率设定为0.005，并在8月和11个时期后减少0.1因素0.1。除非另有指定，否则所有其他超参数均遵循MMDetection中的默认设置[2]。损耗重量λBin设置为1.偏移范围A和箱数N分别设定为3和20。在分层聚焦偏移预测中，阶段K的数量被设置为2。

4.1. Ablation Study

在本节中，我们验证了基线Reset−50−FPN [20]的有效性。没有损失普遍性，我们

Method	AP	AP_{50}	AP_{60}	AP_{70}	AP_{80}	AP_{90}
L_2 Loss [10]	44.7	72.6	67.6	56.8	37.4	7.8
Smooth L_1 Loss [20]						
$\beta = 1.0$	45.0	**74.5**	**69.5**	57.6	36.0	6.6
$\beta = 1.5$	44.3	73.9	68.6	56.5	34.9	6.4
$\beta = 2.0$	44.2	74.3	68.9	56.1	33.9	6.2
Bin Classification	**47.5**	74.0	69.0	**58.8**	**41.5**	**13.6**

Table 2. The effectiveness of different loss functions. β denotes the division point in the $Smooth\ L_1$ loss function. Results are reported on the VOC2007 *test* set [4].

Stage	AP	AP_{50}	AP_{60}	AP_{70}	AP_{80}	AP_{90}
$K = 1$	47.5	**74.0**	**69.0**	58.8	41.5	13.6
$K = 2$	**49.0**	73.2	68.4	**59.0**	**44.3**	**19.6**
$K = 3$	48.8	73.3	68.3	58.5	43.6	19.1

Table 3. The effectiveness of number of stages in the proposed hierarchical focusing offset prediction method. Results are reported on the VOC2007 *test* set [4].

form ablation studies to reveal the effect of each component in our proposed method on the PASCAL VOC dataset [4].

Main Component Analysis. We analyze the effect of each proposed component in Table 1. Simply estimating object localization by the proposed offset bin classification method improves the AP by 0.8% compared with the baseline bounding box regression method [20]. Introducing expectation-based offset prediction and hierarchical focusing offset prediction both achieve gain of 2.5% compared with the baseline, which further boost the prediction precise. The expectation-based offset prediction takes into account the probability of samples in other offset bins to estimate offsets, and consistently improves AP with different IoU metrics. The hierarchical focusing offset prediction performs better in the high IoU metrics. The reason is that it predicts more precise offsets within finer offset bin. Ultimately, our full method outperforms the baseline bounding box regression method by 4.0%. The result demonstrates that the effectiveness of the proposed method in terms of more accurate object detection, especially performing better in the high IoU metrics.

Effectiveness of Different Loss Function for Predicting Offsets. The effectiveness of different loss function for predicting offsets is shown in Table 2. Based on the same backbone network ResNet-50-FPN [20], we adjust the division point β of regression loss $Smooth\ L1$ to make more samples be treated based on enough gradient contributions. However, the detection performance AP is decreased when we set β to a larger value. One possible reason is that the network learning is dominated by some samples with large distance error. Compared with the $Smooth\ L_1$ loss and the L_2 loss, our method performs better performance as shown in Table 2, which alleviates the problem by the offset bin classification.

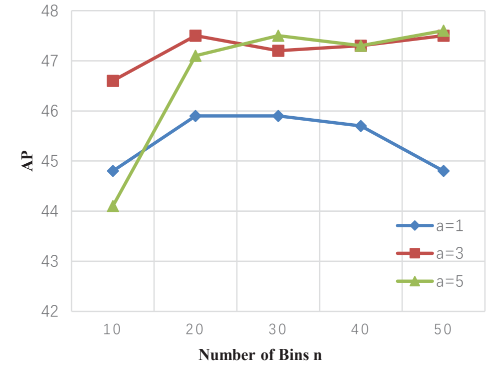

Figure 5. The effectiveness of bin classification for offset bin labels with different hyper-parameters.The horizontal axis represents the number of bins n, the vertical axis stands for detection performance AP. The blue line, the red line and the green line indicate the offset range $a = 1, 3, 5$, respectively.

Setting of Offset Bin Labels. Figure 5 shows the effectiveness of bin classification for offset bin labels with different hyper-parameters. a and n respectively denote the endpoint of the divided offset range and the number of bins. When the number of bins n is fixed, it can be seen that the detection performance is decreased for $a = 1$, while the performance is similar for $a = 3$ and $a = 5$. This is because many samples with offset greater than 1 are ignored during training if $a = 1$. When the endpoint $a = 3$ or 5, it can be observed that the detection performance are very close to each other when the number of bins n is set from 20 to 50, thereby is robust to a long range of offset bin numbers. In addition, the detection performance is relatively poor when n is small (i.e. $n = 10$). To balance the performance with the bin numbers, we choose $a = 3$ and $n = 20$ in our experiments.

Number of Stages in Hierarchical Focusing Offset Prediction. The effectiveness of number of stages in

Method	AP	AP_{50}	AP_{60}	AP_{70}	AP_{80}	AP_{90}
L_2 Loss [10]	44.7	72.6	67.6	56.8	37.4	7.8
Smooth L_1 Loss [20]						
$\beta = 1.0$	45.0	**74.5**	**69.5**	57.6	36.0	6.6
$\beta = 1.5$	44.3	73.9	68.6	56.5	34.9	6.4
$\beta = 2.0$	44.2	74.3	68.9	56.1	33.9	6.2
Bin Classification	**47.5**	74.0	69.0	**58.8**	**41.5**	**13.6**

表2.不同损失功能的有效性。β表示平滑L1损耗功能中的分割点。结果是在VOC2007测试集[4]上报告。

Stage	AP	AP_{50}	AP_{60}	AP_{70}	AP_{80}	AP_{90}
$K = 1$	47.5	**74.0**	**69.0**	58.8	41.5	13.6
$K = 2$	**49.0**	73.2	68.4	**59.0**	**44.3**	**19.6**
$K = 3$	48.8	73.3	68.3	58.5	43.6	19.1

表3.所提出的Hi−批准聚焦偏移预测方法中阶段数量的有效性。结果是在VOC2007测试集[4]上报告。

形成消融研究，以揭示每个组分在Pascal VOC数据集中提出的方法[4]。主要成分分析。我们分析了表1中每个提出的组分的效果1.简单地通过所提出的偏移箱分类方法估算OB−JECT定位，与基线边界盒回归方法相比将AP改善0.8%[20]。介绍基于期望的偏移预测和分层聚焦偏移预测与基线相比，达到2.5%的增益，这进一步提高了预测的预测。基于期望的偏移预测进入AC−计算其他偏移频体中的样本的概率，以便与ES −时分偏移，并一致地改善了不同的IOU度量标准。分层聚焦偏移预测在高IOU度量中执行更好。原因是它在更精细的偏移箱内预测更精确的偏移。Ulti−Menty，我们的完整方法优于基线边界框回归方法4.0%。结果表明，所提出的方法在更准确的对象检测方面的有效性，尤其是在高IOU度量中执行比赛。不同损失函数预测偏移的有效性。表2中所示的不同损失功能的有效性如图2所示。基于相同的骨干网Reset−50−FPN [20]，我们调整回归损耗平滑L1的Di−Vision点β，以便基于处理更多的样品足够的渐变贡献。然而，当我们将β设置为更大的值时，检测性能AP减少。一种可能的原因是网络学习由具有大距离误差的一些样本主导。与光滑的L1损耗和L2损耗相比，我们的方法如图所示执行更好的性能

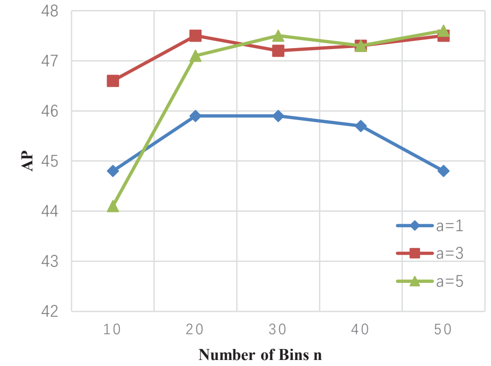

图5.箱体分类对具有不同超参数的偏移箱标签的有效性。横轴表示箱数N，垂直轴代表检测性能AP。蓝线，红线和绿线分别表示偏移量A = 1,3,5。

在表2中，通过偏移箱分类来缓解问题。

偏移箱标签的设置。图5显示了具有不同超参数的偏移箱标签的垃圾箱分类的EF−效力。A和N分别表示分割偏移范围和箱数的终点。当箱数n是固定的时，可以看出，对于a = 1，检测性能降低，而性能类似于a = 3和a = 5。这是因为忽略了大于1的偏移量的许多样本在训练期间，如果a = 1.当端点a = 3或5时，可以观察到当箱n的数量设置为20到50时，检测性能非常靠近，从而坚固到长距离偏移箱数。另外，当n小时，检测性能相对较差（即n = 10）。要使用箱号码平衡性能，我们在实验中选择A = 3和N = 20。

分层聚焦偏移预测中的阶段数。阶段数量的有效性

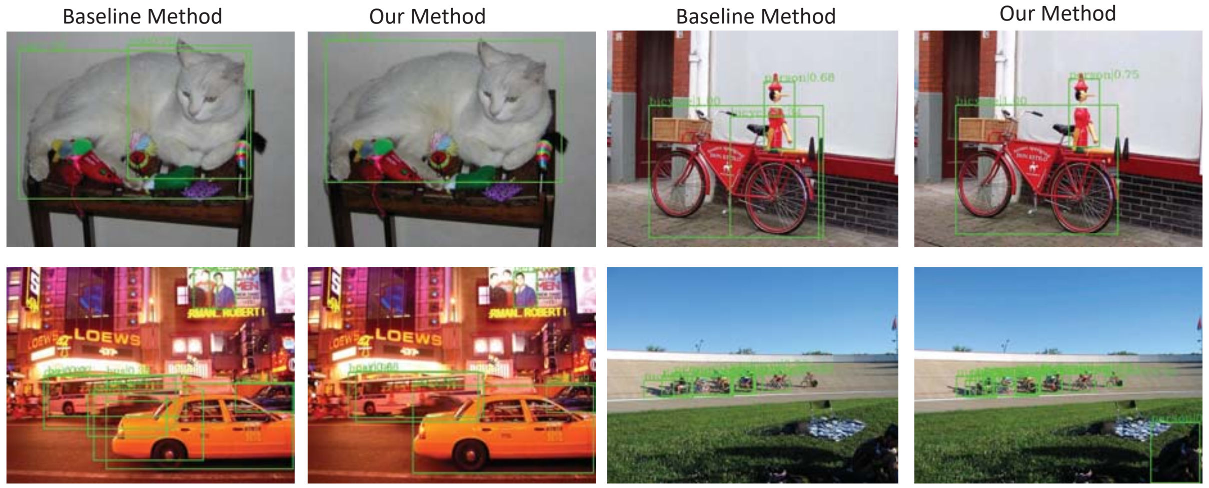

Figure 6. Visualization comparison between the baseline method and the proposed offset bin classification method on the VOC2007 *test* set [4]. The first and third columns show the detection results of the baseline method. The second and fourth columns show that the detection results of our method.

Method	Backbone	AP	AP_{50}	AP_{60}	AP_{70}	AP_{80}	AP_{90}
Faster R-CNN* [35]	ResNet-50-FPN	45.0	**74.5**	**69.5**	57.6	36.0	6.6
Our +Faster R-CNN [35]	ResNet-50-FPN	**49.0**	73.2	68.4	**59.0**	**44.3**	**19.6**
Faster R-CNN* [35]	ResNet-101-FPN	47.8	**75.5**	**70.6**	60.3	41.3	10.5
Our+Faster R-CNN [35]	ResNet-101-FPN	**50.8**	74.0	69.5	**60.8**	**47.2**	**22.5**
Cascade R-CNN* [1]	ResNet-50-FPN	49.5	73.1	**69.0**	**61.0**	45.9	18.1
Our+Cascade R-CNN [1]	ResNet-50-FPN	**50.4**	**73.3**	68.9	60.4	**46.5**	**22.2**
Cascade R-CNN* [1]	ResNet-101-FPN	51.0	73.6	69.6	61.9	48.3	21.1
Our+Cascade R-CNN [1]	ResNet-101-FPN	**51.9**	**73.9**	**69.8**	**62.1**	**48.7**	**25.0**

Table 4. Comparison with state-of-the-art methods on VOC2007 *test* set [4]. The symbol * represents our re-implement results based on MMDetection [2].

hierarchical focusing offset prediction is shown in Table 3. According to the analysis in Figure 5, we set the number of bins n_k in each stage to be same ($n_k = 20$, $k = 1, 2, 3$) and the endpoint $a_1 = 3$ in the first stage. Thus, the end point of offset range a_2 in second stage and a_3 in third stage are set to 0.15 and 0.015, respectively. It can be seen that the detection results AP is improved by 1.6% compared with only one stage when the number of stages $K = 2$. In the second stage, the width of bin is already within a very small range. Adding the third stage, the detection performance is close to the second stage. It can be seen that the bin classification with two stages can achieve the better detection performance.

Visualization Comparison. Figure 6 shows the visualization comparison between the baseline method [20] and the proposed offset bin classification method. It can be observed that the baseline method [20] assigns some bounding boxes that do not tightly surround objects in the first row images of Figure 6, while our method can detect objects more accurately. The second row images of Figure 6 show that the car object and the person object are missed detection in the baseline method [20] due to the low quality bounding boxes.

4.2. Comparison With State-of-the-art Methods

Results on Pascal VOC Dataset. We compare our method with two baselines [1, 20] on VOC2007 *test* set [4] in Table 4. For fair comparison, we adopt the same parameter setting for our method and the corresponding baselines. We replace the bounding box regression network by the proposed method to validate their effectiveness. Because Cascade R-CNN [1] is a multi-stage object detector, we replace the regression branch of each stage in Cascade R-CNN with our offset bin class branch in Figure 2. To reduce the number of parameters, the offset bin classification branch here does not include the hierarchical focusing in Figure 3. We set the

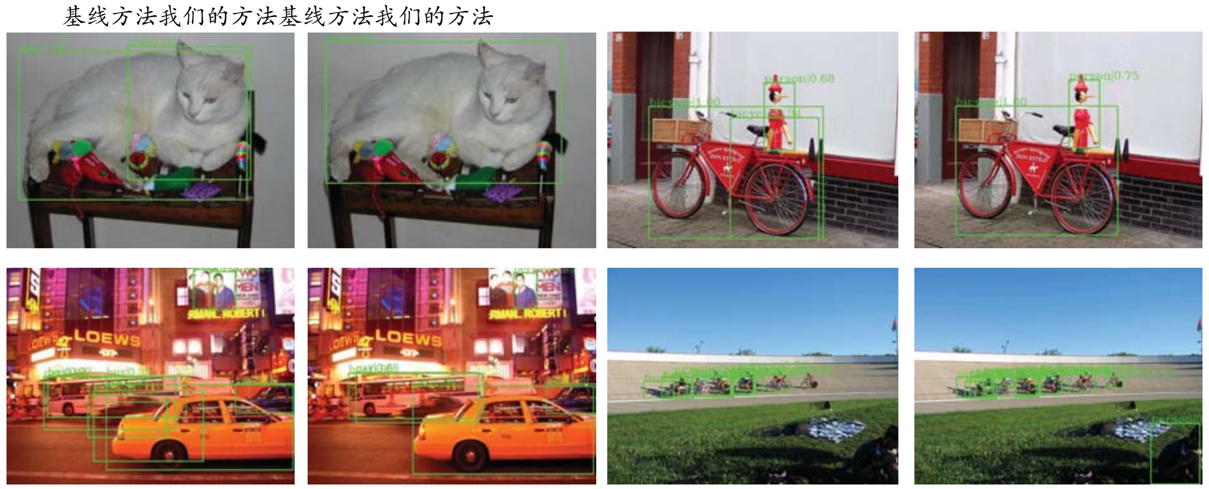

图6.
VOC2007测试集基准方法与建议的偏移箱分类方法之间的可视化比较[4]。第一列和第三列显示基线方法的检测结果。第二个和第四列表明我们方法的检测结果。

Method	Backbone	AP	AP_{50}	AP_{60}	AP_{70}	AP_{80}	AP_{90}
Faster R-CNN* [35]	ResNet-50-FPN	45.0	**74.5**	**69.5**	57.6	36.0	6.6
Our +Faster R-CNN [35]	ResNet-50-FPN	**49.0**	73.2	68.4	**59.0**	**44.3**	**19.6**
Faster R-CNN* [35]	ResNet-101-FPN	47.8	**75.5**	**70.6**	60.3	41.3	10.5
Our+Faster R-CNN [35]	ResNet-101-FPN	**50.8**	74.0	69.5	**60.8**	**47.2**	**22.5**
Cascade R-CNN* [1]	ResNet-50-FPN	49.5	73.1	**69.0**	**61.0**	45.9	18.1
Our+Cascade R-CNN [1]	ResNet-50-FPN	**50.4**	**73.3**	68.9	60.4	**46.5**	**22.2**
Cascade R-CNN* [1]	ResNet-101-FPN	51.0	73.6	69.6	61.9	48.3	21.1
Our+Cascade R-CNN [1]	ResNet-101-FPN	**51.9**	**73.9**	**69.8**	**62.1**	**48.7**	**25.0**

表4.与VOC2007测试集上的最先进方法进行比较[4]。符号⋆代表基于MMDetection [2]的重新实现结果。

分层聚焦偏移预测显示在表3中。根据图5中的分析，我们将每个阶段的箱数NK设置为相同（NK = 20，k = 1,2,3）和端点A1 = 3在第一阶段。因此，第三阶段中的第二级和A3中的偏移范围A2的终点分别设定为0.15和0.015。可以看出，当阶段k = 2的数量时，检测结果AP与仅一个阶段相比提高了1.6%。在第二阶段，箱的宽度已经在非常小的范围内。添加第三阶段，检测性能接近第二级。可以看出，具有两个阶段的BIN分类可以实现更好的检测性能。

可视化比较。图6显示了基线方法[20]与所提出的偏移箱分类方法之间的求助性比较。可以观察到基线方法[20]分配一些不紧密围绕物体的边界框

图6的第一行图像，而我们的方法可以更准确地检测对象。图6的第二行图像显示，由于低质量边界框，在基线方法[20]中错过了汽车对象和人物对象。

4.2。与最先进的方法进行比较

结果Pascal
VOC数据集。我们在表4中将我们使用两个基线[1,20]
[4]上的两个基线[1,20]的方法进行比较。进行公平比较，我们采用了我们的方法和相应基线的相同参数设置。我们通过所提出的方法将边界框回归网络放置验证其有效性。因为Cascade R−CNN
[1]是一个多级对象检测器，所以我们用图2中的胶印箱级分支替换Cascade
R−CNN中每个阶段的再渗起分支。为了减少参数的数量，偏移量宾宾分类分支这里不包括图3中的分层专注。我们设置了

Method	Backbone	AP	AP_{50}	AP_{75}	AP_S	AP_M	AP_L
YOLOv2 [33]	DarkNet-19	21.6	44.0	19.2	5.0	22.4	35.5
SSD512 [23]	ResNet-101	31.2	50.4	33.3	10.2	34.5	49.8
RetinaNet [21]	ResNet-101-FPN	39.1	59.1	42.3	21.8	42.7	50.2
Faster R-CNN [20]	ResNet-101-FPN	36.2	59.1	39.0	18.2	39.0	48.2
Deformable R-FCN [3]	Inception-ResNet-v2	37.5	58.0	40.8	19.4	40.1	52.5
Mask R-CNN [12]	ResNet-101-FPN	38.2	60.3	41.7	20.1	41.1	50.2
Libra R-CNN [28]	ResNet-101-FPN	40.3	61.3	43.9	22.9	43.1	51.0
KL Loss [14]	ResNet-50-FPN	39.2	57.6	42.5	21.2	41.8	52.5
Grid R-CNN [25]	ResNet-101-FPN	41.5	60.9	44.5	23.3	44.9	53.1
IoU-Net [15]	ResNet-101-FPN	40.6	59.0	-	-	-	-
Cascade R-CNN [1]	ResNet-101-FPN	**42.8**	**62.1**	**46.3**	**23.7**	**45.5**	**55.2**
Faster R-CNN* [20]	ResNet-50-FPN	36.6	58.8	39.6	21.6	39.8	45.0
Our+Faster R-CNN	ResNet-50-FPN	**40.5**	**59.6**	**43.1**	**22.6**	**43.1**	**51.0**
Faster R-CNN* [20]	ResNet-101-FPN	38.8	60.9	42.1	22.6	42.4	48.5
Our+Faster R-CNN	ResNet-101-FPN	**42.5**	**61.7**	**45.4**	**23.9**	**45.6**	**53.8**
Faster R-CNN* [20]	ResNeXt-101-FPN	41.9	**63.9**	45.9	**25.0**	45.3	52.3
Our+Faster R-CNN	ResNeXt-101-FPN	**43.2**	62.7	**46.3**	24.7	**46.4**	**54.8**
Cascade R-CNN* [1]	ResNet-50-FPN	40.7	59.3	44.1	23.1	43.6	51.4
Our+Cascade R-CNN	ResNet-50-FPN	**42.3**	**60.4**	**45.8**	**23.9**	**44.8**	**53.6**
Cascade R-CNN* [1]	ResNet-101-FPN	42.4	61.1	46.1	23.6	45.0	54.4
Our+Cascade R-CNN	ResNet-101-FPN	**44.4**	**62.6**	**48.3**	**24.7**	**47.5**	**56.7**
Cascade R-CNN* [1]	ResNeXt-101-FPN	43.7	62.6	47.5	25.3	46.7	55.5
Our+Cascade R-CNN	ResNeXt-101-FPN	**44.7**	**63.1**	**48.5**	**25.3**	**47.8**	**57.1**

Table 5. Comparison with state-of-the-art methods on MS-COCO *test-dev* set [22]. The symbol * represents our re-implement results based on MMDetection [2].

number of stages of Cascade R-CNN to 2. The IoU thresholds are set to 0.5 and 0.7 in the first and second stages, respectively. These baselines are consistently improved by our methods, which demonstrates the advantage and generality of the proposed methods.

Results on MS-COCO Dataset. Furthermore, we also compare the proposed method with some state-of-the-art object detection methods on the large-scale MS-COCO *test-dev* set [22] in Table 5. It can be observed that the proposed method significantly outperforms these state-of-the-art methods. The proposed offset bin classification method can improve the AP of Faster R-CNN [20,35] with ResNet-50-FPN, ResNet-101-FPN and ResNeXt-101-FPN by 3.9%, 3.7% and 1.3%, respectively. The results AP can achieve a considerable accuracy 42.3%, 44.4% and 44.7% when we introduce Cascade R-CNN [1] to our method. The superior performance demonstrates the effectiveness of the proposed offset bin classification method.

5. Conclusion

In this paper, we have proposed an offset bin classification network to achieve more accurate object detection. The offset bin labels construction is first used to discretize the continuous offset into several bins. Then the offset bin classification network predicts the probability distribution of offset bins. Furthermore, the expectation-based offset prediction and the hierarchical focusing offset prediction methods are introduced to turn the discretized classification results into more precise offsets. Our method both achieve superior performance on the PASCAL VOC and MS-COCO object detection datasets. The results demonstrate the effectiveness of our proposed method.

Acknowledgement. This work was supported in part by National Natural Science Foundation of China (No. 61525102, 61831005, 61971095 and 61871078).

References

[1] Zhaowei Cai and Nuno Vasconcelos. Cascade r-cnn: Delving into high quality object detection. In *Proceedings of the IEEE conference on computer vision and pattern recognition*, pages 6154–6162, 2018.

[2] Kai Chen, Jiaqi Wang, Jiangmiao Pang, Yuhang Cao, Yu Xiong, Xiaoxiao Li, Shuyang Sun, Wansen Feng, Ziwei Liu, Jiarui Xu, Zheng Zhang, Dazhi Cheng, Chenchen Zhu, Tian-

Method	Backbone	AP	AP_{50}	AP_{75}	AP_S	AP_M	AP_L
YOLOv2 [33]	DarkNet-19	21.6	44.0	19.2	5.0	22.4	35.5
SSD512 [23]	ResNet-101	31.2	50.4	33.3	10.2	34.5	49.8
RetinaNet [21]	ResNet-101-FPN	39.1	59.1	42.3	21.8	42.7	50.2
Faster R-CNN [20]	ResNet-101-FPN	36.2	59.1	39.0	18.2	39.0	48.2
Deformable R-FCN [3]	Inception-ResNet-v2	37.5	58.0	40.8	19.4	40.1	52.5
Mask R-CNN [12]	ResNet-101-FPN	38.2	60.3	41.7	20.1	41.1	50.2
Libra R-CNN [28]	ResNet-101-FPN	40.3	61.3	43.9	22.9	43.1	51.0
KL Loss [14]	ResNet-50-FPN	39.2	57.6	42.5	21.2	41.8	52.5
Grid R-CNN [25]	ResNet-101-FPN	41.5	60.9	44.5	23.3	44.9	53.1
IoU-Net [15]	ResNet-101-FPN	40.6	59.0	-	-	-	-
Cascade R-CNN [1]	ResNet-101-FPN	**42.8**	**62.1**	**46.3**	**23.7**	**45.5**	**55.2**
Faster R-CNN* [20]	ResNet-50-FPN	36.6	58.8	39.6	21.6	39.8	45.0
Our+Faster R-CNN	ResNet-50-FPN	**40.5**	**59.6**	**43.1**	**22.6**	**43.1**	**51.0**
Faster R-CNN* [20]	ResNet-101-FPN	38.8	60.9	42.1	22.6	42.4	48.5
Our+Faster R-CNN	ResNet-101-FPN	**42.5**	**61.7**	**45.4**	**23.9**	**45.6**	**53.8**
Faster R-CNN* [20]	ResNeXt-101-FPN	41.9	**63.9**	45.9	**25.0**	45.3	52.3
Our+Faster R-CNN	ResNeXt-101-FPN	**43.2**	62.7	**46.3**	24.7	**46.4**	**54.8**
Cascade R-CNN* [1]	ResNet-50-FPN	40.7	59.3	44.1	23.1	43.6	51.4
Our+Cascade R-CNN	ResNet-50-FPN	**42.3**	**60.4**	**45.8**	**23.9**	**44.8**	**53.6**
Cascade R-CNN* [1]	ResNet-101-FPN	42.4	61.1	46.1	23.6	45.0	54.4
Our+Cascade R-CNN	ResNet-101-FPN	**44.4**	**62.6**	**48.3**	**24.7**	**47.5**	**56.7**
Cascade R-CNN* [1]	ResNeXt-101-FPN	43.7	62.6	47.5	25.3	46.7	55.5
Our+Cascade R-CNN	ResNeXt-101-FPN	**44.7**	**63.1**	**48.5**	**25.3**	**47.8**	**57.1**

表5.与MS-COCO测试开发套装上的最先进方法的比较[22]。符号⋆代表基于MMDetection [2]的重新实现结果。

Cascade R-CNN至2的级数分别在第一和第二阶段分别设定为0.5和0.7。这些基线通过我们的方法始终如一地改善，这证明了所提出的方法的优势和赋予。MS-Coco DataSet上的结果。此外，我们还在表5中的大规模MS-Coco Test-Dev集合[22]上的一些最先进的对象检测方法进行了比较了所提出的方法[22]。可以观察到所提出的方法显着优于这些最先进的方法。所提出的偏移箱分类方法可以将Reset-50-FPN，Reset-101-FPN和Resnext-101-FPN的更快R-CNN [20,35]的AP改善为3.9%，3.7%和1.3%。当我们将Cascade R-CNN [1]介绍给我们的方法时，结果AP可以达到相当大的精度42.3%，44.4%和44.7%。优越的性能证明了所提出的偏移箱分类方法的有效性。

5. Conclusion

在本文中，我们提出了一个偏移的垃圾箱分类网络来实现更准确的对象检测。首先使用偏移箱标签结构来将连续偏移分为几个箱。然后，偏移箱分类网络预测偏移箱的概率分布。此外，引入基于期望的偏移预测和分层聚焦偏移预测方法以将离散的分类结果转换为更精确的偏移。我们的方法在Pascal VOC和MS-Coco对象检测数据集中实现了卓越的性能。结果表明了我们所提出的方法的效果。确认。这项工作是由中国国家自然科学基金（61525102,61831005,61971095和61871078号）的支持。

References

[1] Zhaowei Cai和Nuno Vascomcelos。Cascade R-CNN：渗透到高质量的物体检测。在计算机愿景和模式识别的IEEE会议上的诉讼程序中

, pages 6154 6162, 2018. [2] Kai Chen, Jiaqi Wang, Jiangmiao Pang, Yuhang Cao, Yu Xiong, Xiaoxiao Li, Shuyang Sun, Wansen Feng, Ziwei Liu, Jiarui Xu, Zheng Zhang, Dazhi Cheng, Chenchen Zhu, Tian-heng Cheng, Qijie Zhao, Buyu Li, Xin Lu, Rui Zhu, Yue Wu, Jifeng Dai, Jingdong Wang, Jianping Shi, Wanli Ouyang, Chen Change Loy, and Dahua Lin. MMDetection: Open mmlab detection toolbox and benchmark. *arXiv preprint arXiv:1906.07155*, 2019.

[3] Jifeng Dai, Yi Li, Kaiming He, and Jian Sun. R-fcn: Object detection via region-based fully convolutional networks. In *Advances in neural information processing systems*, pages 379–387, 2016.

[4] Mark Everingham, Luc Van Gool, Christopher KI Williams, John Winn, and Andrew Zisserman. The pascal visual object classes (voc) challenge. *International journal of computer vision*, 88(2):303–338, 2010.

[5] Huan Fu, Mingming Gong, Chaohui Wang, Kayhan Batmanghelich, and Dacheng Tao. Deep ordinal regression network for monocular depth estimation. In *Proceedings of the IEEE Conference on Computer Vision and Pattern Recognition*, pages 2002–2011, 2018.

[6] Zhihang Fu, Yaowu Chen, Hongwei Yong, Rongxin Jiang, Lei Zhang, and Xian-Sheng Hua. Foreground gating and background refining network for surveillance object detection. *IEEE Transactions on Image Processing*, 28(12):6077–6090, 2019.

[7] Andreas Geiger, Philip Lenz, and Raquel Urtasun. Are we ready for autonomous driving? the kitti vision benchmark suite. In *2012 IEEE Conference on Computer Vision and Pattern Recognition*, pages 3354–3361. IEEE, 2012.

[8] Spyros Gidaris and Nikos Komodakis. Object detection via a multi-region and semantic segmentation-aware cnn model. In *Proceedings of the IEEE international conference on computer vision*, pages 1134–1142, 2015.

[9] Ross Girshick. Fast r-cnn. In *Proceedings of the IEEE international conference on computer vision*, pages 1440–1448, 2015.

[10] Ross Girshick, Jeff Donahue, Trevor Darrell, and Jitendra Malik. Rich feature hierarchies for accurate object detection and semantic segmentation. In *Proceedings of the IEEE conference on computer vision and pattern recognition*, pages 580–587, 2014.

[11] Jicheng Gong, Zhao Zhao, and Nic Li. Improving multi-stage object detection via iterative proposal refinement.

[12] Kaiming He, Georgia Gkioxari, Piotr Dollár, and Ross Girshick. Mask r-cnn. In *Proceedings of the IEEE international conference on computer vision*, pages 2961–2969, 2017.

[13] Kaiming He, Xiangyu Zhang, Shaoqing Ren, and Jian Sun. Deep residual learning for image recognition. In *Proceedings of the IEEE conference on computer vision and pattern recognition*, pages 770–778, 2016.

[14] Yihui He, Chenchen Zhu, Jianren Wang, Marios Savvides, and Xiangyu Zhang. Bounding box regression with uncertainty for accurate object detection. In *Proceedings of the IEEE Conference on Computer Vision and Pattern Recognition*, pages 2888–2897, 2019.

[15] Borui Jiang, Ruixuan Luo, Jiayuan Mao, Tete Xiao, and Yuning Jiang. Acquisition of localization confidence for accurate object detection. In *Proceedings of the European Conference on Computer Vision (ECCV)*, pages 784–799, 2018.

[16] Hei Law and Jia Deng. Cornernet: Detecting objects as paired keypoints. In *Proceedings of the European Conference on Computer Vision (ECCV)*, pages 734–750, 2018.

[17] Buyu Li, Wanli Ouyang, Lu Sheng, Xingyu Zeng, and Xiaogang Wang. Gs3d: An efficient 3d object detection framework for autonomous driving. In *Proceedings of the IEEE Conference on Computer Vision and Pattern Recognition*, pages 1019–1028, 2019.

[18] Wei Li, Hongliang Li, Qingbo Wu, Xiaoyu Chen, and King Ngi Ngan. Simultaneously detecting and counting dense vehicles from drone images. *IEEE Transactions on Industrial Electronics*, 66(12):9651–9662, 2019.

[19] Wei Li, Hongliang Li, Qingbo Wu, Fanman Meng, Linfeng Xu, and King Ngi Ngan. Headnet: An end-to-end adaptive relational network for head detection. *IEEE Transactions on Circuits and Systems for Video Technology*, 2019.

[20] Tsung-Yi Lin, Piotr Dollár, Ross Girshick, Kaiming He, Bharath Hariharan, and Serge Belongie. Feature pyramid networks for object detection. In *Proceedings of the IEEE conference on computer vision and pattern recognition*, pages 2117–2125, 2017.

[21] Tsung-Yi Lin, Priya Goyal, Ross Girshick, Kaiming He, and Piotr Dollár. Focal loss for dense object detection. In *Proceedings of the IEEE international conference on computer vision*, pages 2980–2988, 2017.

[22] Tsung-Yi Lin, Michael Maire, Serge Belongie, James Hays, Pietro Perona, Deva Ramanan, Piotr Dollár, and C Lawrence Zitnick. Microsoft coco: Common objects in context. In *European conference on computer vision*, pages 740–755. Springer, 2014.

[23] Wei Liu, Dragomir Anguelov, Dumitru Erhan, Christian Szegedy, Scott Reed, Cheng-Yang Fu, and Alexander C Berg. Ssd: Single shot multibox detector. In *European conference on computer vision*, pages 21–37. Springer, 2016.

[24] Wei Liu, Shengcai Liao, and Weidong Hu. Perceiving motion from dynamic memory for vehicle detection in surveillance videos. *IEEE Transactions on Circuits and Systems for Video Technology*, 2019.

[25] Xin Lu, Buyu Li, Yuxin Yue, Quanquan Li, and Junjie Yan. Grid r-cnn. In *Proceedings of the IEEE Conference on Computer Vision and Pattern Recognition*, pages 7363–7372, 2019.

[26] Mahyar Najibi, Mohammad Rastegari, and Larry S Davis. G-cnn: an iterative grid based object detector. In *Proceedings of the IEEE conference on computer vision and pattern recognition*, pages 2369–2377, 2016.

[27] Alejandro Newell and Jia Deng. Pixels to graphs by associative embedding. In *Advances in neural information processing systems*, pages 2171–2180, 2017.

[28] Jiangmiao Pang, Kai Chen, Jianping Shi, Huajun Feng, Wanli Ouyang, and Dahua Lin. Libra r-cnn: Towards balanced learning for object detection. In *Proceedings of the IEEE Conference on Computer Vision and Pattern Recognition*, pages 821–830, 2019.

[29] Adam Paszke, Sam Gross, Soumith Chintala, Gregory Chanan, Edward Yang, Zachary DeVito, Zeming Lin, Alban Desmaison, Luca Antiga, and Adam Lerer. Automatic differentiation in pytorch. 2017.

heng Cheng, Qijie Zhao, Buyu Li, Xin Lu, Rui Zhu, Yue Wu, Jifeng Dai, Jingdong Wang, Jianping Shi, Wanli Ouyang, Chen Change Loy, and Dahua Lin. MMDetection: Open mmlab detection toolbox and benchmark. arXiv preprint arXiv:1906.07155, 2019. [3] Jifeng Dai, Yi Li, Kaiming He, and Jian Sun. R−fcn: Object detection via region−based fully convolutional networks. In Advances in neural information processing systems, pages 379   387, 2016. [4] Mark Everingham, Luc Van Gool, Christopher KI Williams, John Winn, and Andrew Zisserman. The pascal visual object classes (voc) challenge. International journal of computer vision, 88(2):303   338, 2010. [5] Huan Fu, Mingming Gong, Chaohui Wang, Kayhan Bat− manghelich, and Dacheng Tao. Deep ordinal regression net− work for monocular depth estimation. In Proceedings of the IEEE Conference on Computer Vision and Pattern Recogni− tion, pages 2002   2011, 2018. [6] Zhihang Fu, Yaowu Chen, Hongwei Yong, Rongxin Jiang, Lei Zhang, and Xian−Sheng Hua. Foreground gating and background refining network for surveillance object detec− tion. IEEE Transactions on Image Processing, 28(12):6077   6090, 2019. [7] Andreas Geiger, Philip Lenz, and Raquel Urtasun. Are we ready for autonomous driving? the kitti vision benchmark suite. In 2012 IEEE Conference on Computer Vision and Pattern Recognition, pages 3354   3361. IEEE, 2012. [8] Spyros Gidaris and Nikos Komodakis. Object detection via a multi−region and semantic segmentation−aware cnn model. In Proceedings of the IEEE international conference on com− puter vision, pages 1134   1142, 2015. [9] Ross Girshick. Fast r−cnn. In Proceedings of the IEEE inter− national conference on computer vision, pages 1440   1448, 2015. [10] Ross Girshick, Jeff Donahue, Trevor Darrell, and Jitendra Malik. Rich feature hierarchies for accurate object detection and semantic segmentation. In Proceedings of the IEEE con− ference on computer vision and pattern recognition, pages 580   587, 2014. [11] Jicheng Gong, Zhao Zhao, and Nic Li. Improving multi− stage object detection via iterative proposal refinement. [12] Kaiming He, Georgia Gkioxari, Piotr Doll   ar, and Ross Gir− shick. Mask r−cnn. In Proceedings of the IEEE international conference on computer vision, pages 2961   2969, 2017. [13] Kaiming He, Xiangyu Zhang, Shaoqing Ren, and Jian Sun. Deep residual learning for image recognition. In Proceed− ings of the IEEE conference on computer vision and pattern recognition, pages 770   778, 2016. [14] Yihui He, Chenchen Zhu, Jianren Wang, Marios Savvides, and Xiangyu Zhang. Bounding box regression with uncer− tainty for accurate object detection. In Proceedings of the IEEE Conference on Computer Vision and Pattern Recogni− tion, pages 2888   2897, 2019. [15] Borui Jiang, Ruixuan Luo, Jiayuan Mao, Tete Xiao, and Yun− ing Jiang. Acquisition of localization confidence for accurate object detection. In Proceedings of the European Conference on Computer Vision (ECCV), pages 784   799, 2018.

[16]嘿法律和贾邓。

Cornernet：将对象检测为配对键点。在欧洲经验（ECCV）上的欧洲会议上，第734−750,2018页。[17] Buyu Li，Wanli欧阳，陆胜，兴宇曾和小刚王。

GS3D：高效的3D对象检测帧 −

用于自主驾驶。在IEEE电脑愿景和模式识别会议上的诉讼程序中，第1019−1028,2019页。[18] Wei Li，Hongliang Li，青佛吴，孝感和国王Ng。同时从寄生虫图像中检测和计数密集的车辆。

IEEE工业电子产品交易，66（12）：2019年9651−9662，2019年。[19]魏丽，宏良李，青湾吴，凡人猛，林峰徐和王朝王。

Headnet：用于头部检测的端到端自适应关系网络。视频技术电路和系统的IEEE交易，2019年。特征用于对象检测的PYRA−中途网络。在IEEE计算机愿景和模式识别上的IEEE会议上，第2117−2125,2017页。[21] Tsung−yi Lin，Priya Goyal，Ross Girshick，Kaiming He和Piotr

Doll'ar。致密物体检测的焦损。在IEEE国际计算机愿景会议上，2017年第2980−2988,2017页。[22] Tsung−yi Lin，Michael Maire，Serge Ipplie，James Hays，Pietro Perona，Deva Ramanan，Piotr Doll'ar和C劳伦斯Zitnick。

Microsoft

Coco：上下文中的常见对象。在欧洲计算机愿景会议上，第740−755页。斯普林斯，2014年。[23]魏刘，龙玉米武奴罗维尔州，Dumitru Erhan，Christian Szegedy，Scott Reed，Cheng−Yang Fu和Alexander C Berg。

SSD：单次拍摄多杆探测器。在欧洲在电脑愿景中的影响，第21−37页。

Springer，2016年。[24]魏刘，胜凯辽，和威勇湖。感知动态存储器的车辆检测中的动态记忆。电路技术的IEEE交易，用于视频技术，2019年。[25]鑫璐，李丽，玉溪悦，泉泉李，俊杰燕。网格R−CNN。在IEEE愿景和模式识别的IEEE会议上，2019年7363−7372,2019。[26] Mahyar Najibi，Mohammad Rastegari和Larry S Davis。

G−CNN：基于迭代网格的物体检测器。在电脑愿景和模式识别上的IEEE会议上的记录中，第2369−2377,2016页。[27] Alejandro Newell和Jia Deng。

Assocatia嵌入到图形的像素。在神经信息处理系统的进步中，2017年第2171−2180,2017页。[28]江米庞，开辰，建平史，华军冯，万利欧阳和大华林。天秤座R−CNN：朝着对象检测的禁止学习。在计算机愿景和模式识别上的IEEE会议上，第821−830,2019页。[29] Adam Paszke，Sam Gross，Soumith Chintala，Gregory Chanan，Edward Yang，Zachary Devito，Zeming Lin，Al−Ban Desmaison，luca antiga和adam lerer。 Pytorch中的自动差异化。

2017年。

[30] Heqian Qiu, Hongliang Li, Qingbo Wu, Fanman Meng, King Ngi Ngan, and Hengcan Shi. A2rmnet: Adaptively aspect ratio multi-scale network for object detection in remote sensing images. *Remote Sensing*, 11(13):1594, 2019.

[31] Heqian Qiu, Hongliang Li, Qingbo Wu, Fanman Meng, Linfeng Xu, King N Ngan, and Hengcan Shi. Hierarchical context features embedding for object detection. *IEEE Transactions on Multimedia*, 2020.

[32] Joseph Redmon, Santosh Divvala, Ross Girshick, and Ali Farhadi. You only look once: Unified, real-time object detection. In *Proceedings of the IEEE conference on computer vision and pattern recognition*, pages 779–788, 2016.

[33] Joseph Redmon and Ali Farhadi. Yolo9000: better, faster, stronger. In *Proceedings of the IEEE conference on computer vision and pattern recognition*, pages 7263–7271, 2017.

[34] Joseph Redmon and Ali Farhadi. Yolov3: An incremental improvement. *arXiv preprint arXiv:1804.02767*, 2018.

[35] Shaoqing Ren, Kaiming He, Ross Girshick, and Jian Sun. Faster r-cnn: Towards real-time object detection with region proposal networks. In *Advances in neural information processing systems*, pages 91–99, 2015.

[36] Hamid Rezatofighi, Nathan Tsoi, JunYoung Gwak, Amir Sadeghian, Ian Reid, and Silvio Savarese. Generalized intersection over union: A metric and a loss for bounding box regression. In *Proceedings of the IEEE Conference on Computer Vision and Pattern Recognition*, pages 658–666, 2019.

[37] Rasmus Rothe, Radu Timofte, and Luc Van Gool. Dex: Deep expectation of apparent age from a single image. In *Proceedings of the IEEE International Conference on Computer Vision Workshops*, pages 10–15, 2015.

[38] Hengcan Shi, Hongliang Li, Fanman Meng, and Qingbo Wu. Key-word-aware network for referring expression image segmentation. In *Proceedings of the European Conference on Computer Vision (ECCV)*, pages 38–54, 2018.

[39] Hengcan Shi, Hongliang Li, Fanman Meng, Qingbo Wu, Linfeng Xu, and King Ngi Ngan. Hierarchical parsing net: Semantic scene parsing from global scene to objects. *IEEE Transactions on Multimedia*, 20(10):2670–2682, 2018.

[40] Hengcan Shi, Hongliang Li, Qingbo Wu, Fanman Meng, and King N Ngan. Boosting scene parsing performance via reliable scale prediction. In *Proceedings of the 26th ACM international conference on Multimedia*, pages 492–500, 2018.

[41] Hengcan Shi, Hongliang Li, Qingbo Wu, and Zichen Song. Scene parsing via integrated classification model and variance-based regularization. In *Proceedings of the IEEE Conference on Computer Vision and Pattern Recognition*, pages 5307–5316, 2019.

[42] Bugra Tekin, Sudipta N Sinha, and Pascal Fua. Real-time seamless single shot 6d object pose prediction. In *Proceedings of the IEEE Conference on Computer Vision and Pattern Recognition*, pages 292–301, 2018.

[43] Zhi Tian, Chunhua Shen, Hao Chen, and Tong He. Fcos: Fully convolutional one-stage object detection. In *Proceedings of the IEEE International Conference on Computer Vision*, pages 9627–9636, 2019.

[44] Bin Yang, Junjie Yan, Zhen Lei, and Stan Z Li. Craft objects from images. In *Proceedings of the IEEE Conference on Computer Vision and Pattern Recognition*, pages 6043–6051, 2016.

[45] Tsun-Yi Yang, Yi-Ting Chen, Yen-Yu Lin, and Yung-Yu Chuang. Fsa-net: Learning fine-grained structure aggregation for head pose estimation from a single image. In *Proceedings of the IEEE Conference on Computer Vision and Pattern Recognition*, pages 1087–1096, 2019.

[46] Jiahui Yu, Yuning Jiang, Zhangyang Wang, Zhimin Cao, and Thomas Huang. Unitbox: An advanced object detection network. In *Proceedings of the 24th ACM international conference on Multimedia*, pages 516–520. ACM, 2016.

[47] Xingyi Zhou, Dequan Wang, and Philipp Krähenbühl. Objects as points. *arXiv preprint arXiv:1904.07850*, 2019.

[30]鹤倾秋，弘良李，青江吴，樊曼·孟，国王Nggn，恒
申史。
A2RMNET：遥感图像中的对象检测的自适应方式多尺度
网络。遥感，11（13）：1594,2019。[31]贺倩邱，弘良李
，青武，樊曼梦，林峰徐，国王，恒河史。分层配置文件
嵌入用于对象检测。 Muremedia，2020年的IEEE经交。[32]
Joseph Redmon，Santosh Divvala，Ross Girshick和Ali
Farhadi。你只看一次：统一，实时对象模式。在电脑愿景
和模式识别的IEEE会议上的讨论中，2016年779–788，[33]
Joseph Redmon和Ali Farhadi。
YOLO9000：更好，更快，更强。在计算机愿景和模式识
别的IEEE会议上的讨论中，2017年7263–7271,2017。[34]
Joseph Redmon和Ali Farhadi。 YOLOV3：增量改进。
Arxiv预印迹arxiv：1804.02767,2018。[35]邵庆仁，凯明，
罗斯吉伦克和剑孙。
R–CNN更快：与区域提案网络的实时对象检测。在神经
信息的进展中，2015年第91–99页的第91–99页。联盟的广
义概括：界限框回归的度量和损失。在IEEE愿景和模式识
别的IEEE会议上，2019年658–666,2019。[37] Rasmus
Rothe，Radu Timofte和Luc Van
Gool。德克斯：从单一形象的明显年龄的深入期望。在IEE
E电脑视觉研讨会上的验收中，2015年10–15，第10–15页
的第10–15页。[38]恒珊史，河江李，樊曼孟，青武。用于
引用表达式图像段的密钥 –
字感知网络。在欧洲电脑愿景（ECCV）会议上，第38–54
页，2018年第38–54页。[39]恒珊史，洪良李，樊曼孟，青
博吴，林峰徐和王尼吉。分层解析网：从全局场景解析对
象的语义场景。多媒体的IEEE交易，20（10）：2670–268
2,2018。[40]恒珊施，洪良李，青博武，樊曼蒙和国王Ng。
通过可释放的预测提高场景解析性能。在第26届ACM国际
多媒体会议上，第492–500页，2018年第492–500页。[41]
恒珊史，弘良李，青武和淄博宋。通过集成分类模型和基
于方差的正规解析场景解析。在IEEE计算机愿景和模式识
别会议上的诉讼程序中，2019年第5307–5316页，2019年。
[42] Bugra Tekin，Sudipta Ninha和Pascal
Fua。实时无缝单射6D对象姿态预测。在计算机愿景和模
式识别上的IEEE会议上的报告中，第292–301,2018页。[43]
志田，春华沉，郝辰和童。
FCOS：完全卷积的单阶段对象检测。在IEEE计算机舞台
上的IEEE国际会议上的报告中，2019年9627–9636，[44]斌
杨，朱杰燕，镇磊和斯坦Z李。从图像中的曲目。在IEEE
会议的诉讼中

在电脑视觉和模式识别上，第6043–6051,2016,2016。[45]
Tsun–yi Yang，Yi–Ting Chen，Yen–Yu Lin和Yung–yu
Chuang。FSA–NET：从单个图像中学习头部姿势估计的
细粒度结构聚合。在计算机愿景和模式识别上的IEEE会议
上，2019年1087–1096，2019年第1087–1096页。[46]嘉徽
宇，云宁江，张阳王，志宁曹，托马斯黄。UnitBox：高级
对象检测网络。在第24届ACM国际会议上关于多媒体，第
516–520页的法律程序。ACM，2016. [47]兴义周，Dequan
Wang和PhilippKr ¨ ahenb ¨ uhl。ob–jects作为积分。Arxiv预
印迹Arxiv：1904.07850,2019。